LAWRENCE
LIVERMORE
NATIONAL
LABORATORY

UCRL-TR-207361

# Fabrication and Characterization of Graded Cu-Doped Be Shells - Details and Documentation of Our First Attempt

J. Gunther, M. McElfresh, C. Alford, H. Huang, R. Cook

October 20, 2004

This work was performed under the auspices of the U.S. Department of Energy by University of California, Lawrence Livermore National Laboratory under Contract W-7405-Eng-48.

***Target Area Technologies Program***

*Mail Station L-481*

*Ext: 2-3117*

**Date:** October 12, 2004

**To:** Distribution

**From:** Janelle Gunther, Mike McElfresh, Craig Alford, Haibo Huang (GA), Bob Cook

**Subject:** Fabrication and Characterization of Graded Cu-doped Be Shells - Details and Documentation of Our First Attempt

## Summary

We have fabricated by sputtering and characterized a set of step-graded Cu-doped Be capsules. The capsules were made with Cu doped layers of about 0.35 and 0.70 atom % Cu. The total thickness of the coating is about 100 µm. Capsules were removed from the coater for characterization after each layer was deposited. Our ability to produce doped layers is confirmed, and our ability to control the level of doping is excellent. A variety of characterization techniques, both destructive and non-destructive were explored. The surface finish of the sample capsules removed after each layer progressively got rougher, it is likely that polishing will be necessary to produce capsules that will meet surface specifications. We have learned a great deal from this first effort, both in terms of coating technology and capsule characterization. We are now implementing several changes in the coating system based in part upon our experience with this first effort. The next graded capsule run should begin near the end of October.

## Introduction

In the last year much has changed in the ICF program. What has motivated the work detailed in *this* memo is a new capsule design[1] that uses a graded dopant, in this case Cu in Be, to suppress the acceleration phase Rayleigh-Taylor instability coming from medium and high frequency capsule surface roughness, thus leading to a much more robust capsule. A schematic of the design is shown in Figure 1.[2]

To fabricate the empty target we sputter Be onto a plastic mandrel, which is then later removed thermally through what will be the fill hole.[3] To make the Cu-doped layers, a small Cu sputter gun is used in tandem with the Be sputter guns. Relative control of the power to the guns allows the control of the Cu concentration in the final target.

---

[1] S. W. Haan, et al., "Update on the NIF Indirect Drive Ignition Target Fabrication Specifications," *Fusion Sci. and Technol.* **45**, 69 (2004). Similar designs have since been developed for Ge doped CH.

[2] Taken directly from Ref 1.

[3] B. Cook, S. Letts, and S. Buckley, "Experimental confirmation of CH mandrel removal from Be shells," LLNL Internal Memo, June 8, 2004. Copy available from Bob Cook.

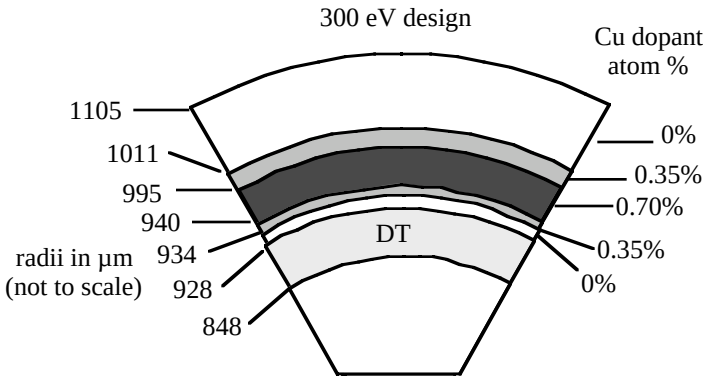


Ablator roughness specs on four designs

| $T_R$ (eV) | $E_{abs}$ (kJ) | max Cu% | ablator rms |
|---|---|---|---|
| 250 | 115 | 0.35% | 7 nm |
| 250 | 300 | 0.35% | 100 nm |
| 250 | 700 | 0.35% | 280 nm |
| 300 | 200 | 0.70% | 220 nm |

**Figure 1.** Be capsule with graded Cu dopant. The Be next to the DT fuel is undoped, the dopant rises to a maximum in two steps and then back down again. The 300 eV design is shown. The 250 eV designs are scales of the design by Dittrich[4]. The table shows the allowed ablator rms roughness (1/3 of the ablator perturbation that causes 50% yield degradation, in modes 12 and above).

Previously we have fabricated a number of relatively thin walled (~20-30 μm) capsules with constant Cu concentration, and one capsule run (with a constant level of Cu doping) to a thickness of near 100 μm. Thus our fabrication challenges were three-fold. First, could we control the Cu concentration at levels near to what is required; second, could we change the Cu concentration to provide steps like are shown in figure 1, and third could we combine the first two elements to produce a NIF thickness capsule. Added to these challenges were the problems associated with characterization. In this report we document our first efforts at meeting these objectives. Rather than try to completely duplicate the design of Figure 1, we instead tried to match the desired concentrations but in layers that were of thicknesses that would make the development of characterization tools easier. The details of the fabrication and subsequent characterization are described below.

## Fabrication

The Cu-doped Be capsules were prepared by sputtering using separate Cu and Be sources. As shown in Figures 2 and 3, four 2-inch MAC sputter guns arranged on a square were used to sputter pure Be. A 1.3-inch mini-MAC sputter gun centered between the four Be guns was used to sputter Cu. The bounce pan is driven by a piezo-electric drive mechanism using an amplified Wavetek signal source. The bounce frequency is repeatedly cycled from 15 to 20 kHz over 0.05 second intervals. All sputtering was done in a 3.7 mTorr Argon atmosphere. The gas is introduced into the sputter chamber via a flanged path in front of the camera port. This allows the camera port to remain clean.

[4] T. R. Dittrich, et al., "Reduced Scale National Ignition Facility Capsule Design," *Phys. Plasmas* **5**, 3708 (1998).

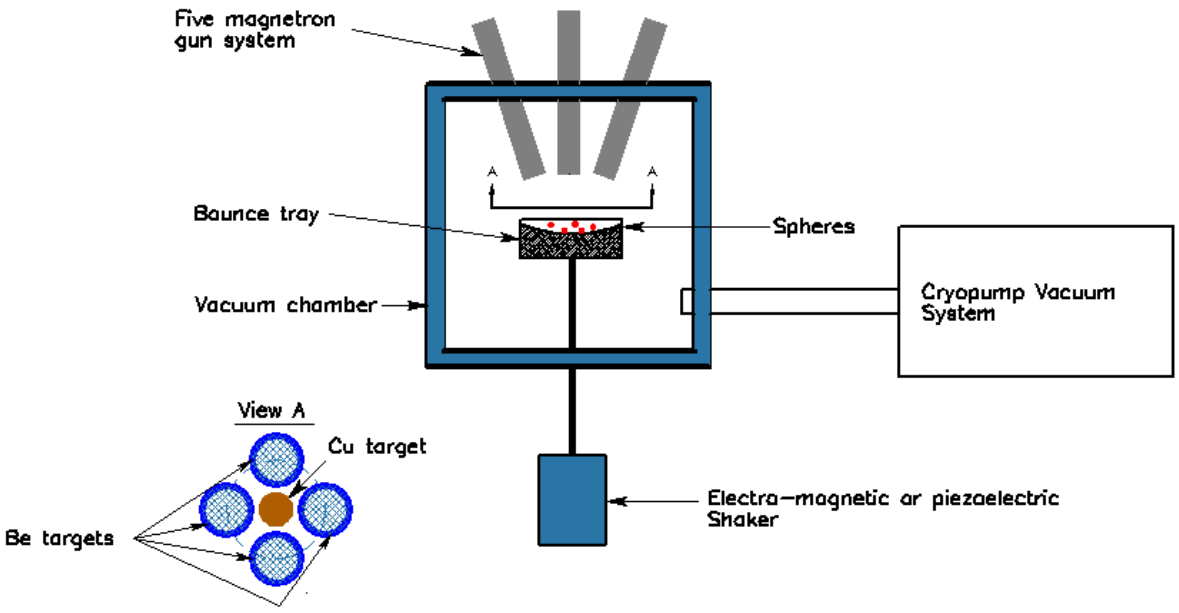


**Figure 2.** Schematic diagram of the Be sputter system. Four MAC 2-inch sputter guns arranged on a square are used to sputter the pure Be, while a single 1.3-inch MAC gun is used to sputter Cu. A piezoelectric driver is used to drive the pan in order to keep the capsules in motion.

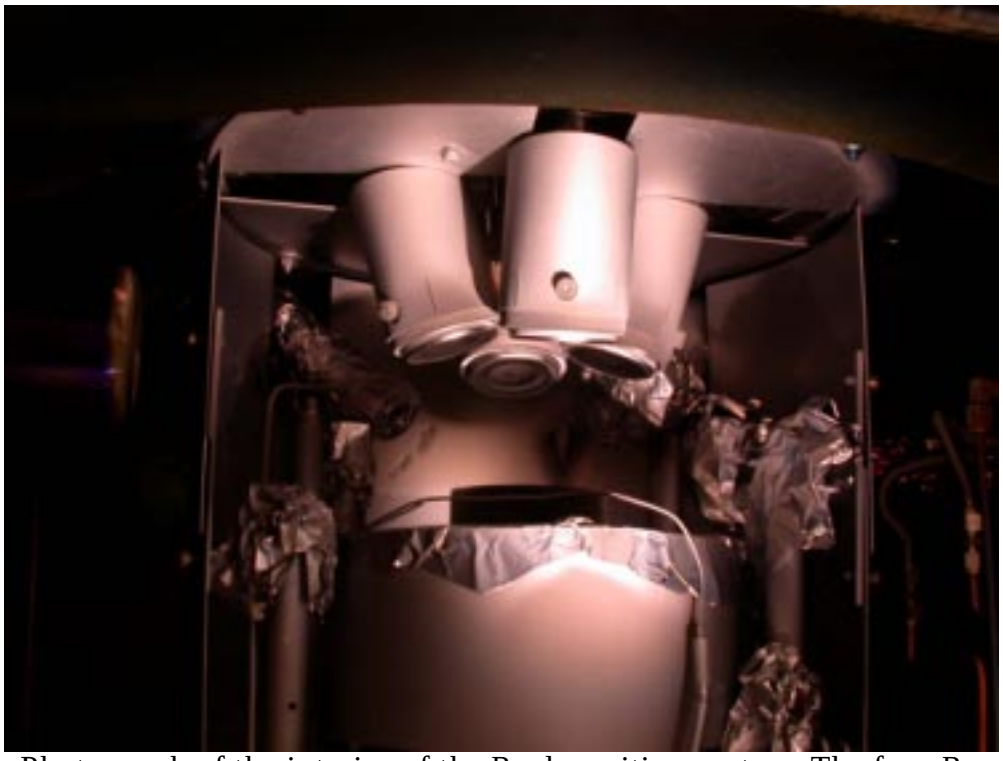

**Figure 3.** Photograph of the interior of the Be deposition system. The four Be guns are evident a well as the bounce pan.


**Figure 4.** Bounce pans used for sputter coating. The pan on the left is used during the Be precoat, with up to eight capsules constrained to the dimples evident in the photo. The pan on the right is currently used when coating with up to twenty-four precoated capsules loaded. The pan the middle has a screen rather than a solid surface in order to allow debris to fall through rather than collect in the pan. All pans are mounted to a structure to minimize or eliminate resonance modes.

For the full thickness run, eight 2-mm-diameter ~12 µm walled CH-mandrels were loaded into the "dimples" of the precoat bounce pan shown in Figure 4. After pumping the system overnight to a base pressure in the $10^{-8}$ range, the capsules were precoated with about 0.1 µm pure Be using two Be sputter sources each operating at approximately 40 to 50-watts for 1 hour. The bounce pan was electrically floating with respect to ground during the precoating runs.

After precoating three batches of capsules, the bounce pan was changed to an undimpled pan (see Figure 4) and twenty-three capsules were then loaded for the full thickness coating runs. During these depositions the Be sputter sources were operated at 300 watts each. The copper source was operated at its lowest reliable power level of 4 watts during the 0.35 atom % Cu deposition and at 8 watts during the 0.70 atom % Cu deposition. In addition, a 0.4 inch aperture was mounted at the output of the Cu gun in order to further reduce the Cu flux. An electrical bias of 80 volts is applied between the bounce pan and ground during the Be/Be-Cu deposition. After pumping the system overnight to a base pressure in the $10^{-8}$ range the capsules were coated with pure Be for two days to a thickness of 18 µm, then at a target Cu doping value of 0.35 atom % for two days for a layer thickness of 18 µm, then 0.70 atom % for three days for a layer

thickness of 27 µm, and then 0.35 atom % for another three days for a layer thickness of 27 µm. The deposition chamber was opened and three capsules were removed after the layer of each composition was complete. In addition, after opening the deposition chamber the system was pumped overnight to a base pressure in the $10^{-8}$ range. The final layer was to be pure Be, however on the second day of pure Be deposition it was observed that the capsules were not bouncing in the bounce pan. Debris accumulated in the pan and was sticking to the capsule surfaces and the capsules were observed to become very rough (dull / diffusive scattering) in appearance. The bounce pan drive amplifier was modified in order to roughly double the drive power and the capsules were rerun. However, the capsules still did not bounce and the run was terminated. Shown in Figure 11 in the Characterization section below is an electron microscope image of a polished section of the final Cu-doped Be capsule wall showing the various layers. The light colored lines spaced at about 9 µm are attributed to oxidation of the shells after the sputtering is turned off at the end of a workday. There will be more discussion about this below.

Calibrations of the Cu-doping level were undertaken prior to making the thick capsules. The Cu sputter gun power level was approximated using chemical composition results from XRF measurements made on flat samples. In separate runs capsule mandrels were coated with Be-Cu at target doping values of 0.35 atom % and 0.70 atom %. The capsules then were sent out for neutron activation analysis in order to get an absolute calibration of the composition. The values of Cu-doping were found to be 0.33 atom % and 0.65 atom %, close to the desired values. A more detailed discussion is included in the Characterization section below. Efforts to carefully control the Cu content will be delayed until we have further optimized the deposition system.

Several years ago it was observed that capsules would deform if they were directly exposed to the full output power of the Be sputter guns. In order to accommodate this observation typically the four Be sputter heads are ramped up to full power of 300 watts over several tens of minutes (i.e. 30 to 60 minutes). However, since the Cu sputter source is always operated near its lowest power setting it is not ramped but rather is maintained at the final operating setting as the Be sources ramp up. The consequence of this procedure is that the Cu content will be too high when the Be sources are being ramped. Figure 5 shows the Cu composition measured by electron probe as a function of position. (There is more discussion of the characterization technique below.) It can be seen that there are excursions in the Cu content at the start of deposition runs. In order to address this, a shutter is being incorporated into the new bottom flange of the deposition chamber. Tests will be run with the shutter closed during the power ramp in order to see if the capsules can tolerate rapid exposure to the full power output of the sources. Because the capsules will now have at least 6 µm of Be before they are subjected to the heat pulse associated with opening the shutter there may not be an issue for the current operating situation. If successful, the shutter will be used in future runs. If the current shutter type does not work (i.e. capsules deform) we will pursue the use of another type of shutter that opens gradually allowing the power to which the capsules are exposed to be ramped up while the Be and Cu sources run at their final power conditions.

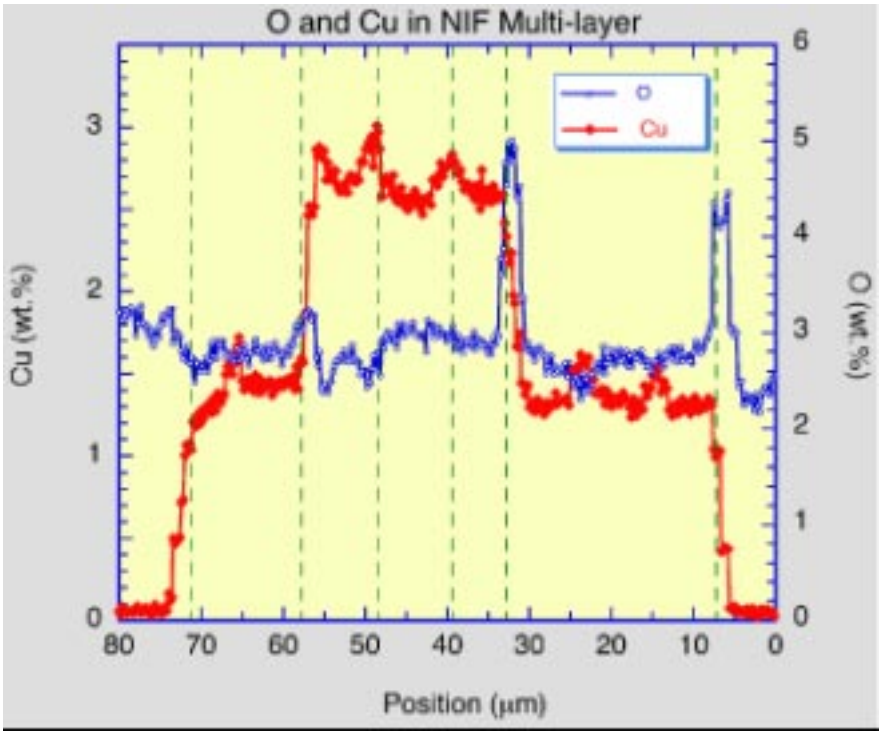


**Figure 5.** Copper and oxygen composition as a function of position as determined by electron probe. Position zero refers to the outer surface of the capsule.

Also shown in Figure 5 are peaks in the oxygen composition at some of the regions of interfaces between compositions, a feature also seen in the SEM of the polished wall cross-section shown in Figure 11. The layer at each interface has been observed previously and is probably a result of shutting down the deposition every day. The larger peaks in Figure 5 appear to be associated with points at which the chamber was opened in order to remove capsules and regenerate the sputter heads. The system is run only during the day in order to allow constant human monitoring of the deposition, since failures have occurred in the past (e.g. capsules welding to each other and capsules bouncing out of the pan). Achieving continuous, unmonitored running conditions is a high priority objective for FY05.

A new drive mechanism for the bounce pan is currently being incorporated into the sputter chamber to address the problems with the previous drive. This will be done by modifying the flange on the bottom of the deposition chamber to accommodate both a new speaker-type (electromagnetic) mechanical drive and the current piezoelectric drive. In addition the flange will accommodate a shutter mechanism for reasons to be discussed below.

## Characterization

A successful ignition campaign will depend in part upon having highly characterized capsules. Properties of interest include symmetry, surface features, microstructure, chemical composition and strength. Although there is an emphasis on non-destructive testing, a number of destructive tests were used to provide critical information for process development and improvement. As noted above, three capsules were removed after deposition of each major layer and reserved exclusively for characterization.

One of the most critical and obvious issues is that of surface roughness and morphology. This is one of the areas in which very specific and tight tolerances are specified. The surface morphology was studied both with Scanning Electron Microscopy (SEM) and Sphere-mapping. In SEM, incident electrons from the filament ionize the sample and produce a vacancy in the inner shell. When the atom decays from its excited state, it produces either a characteristic photon (x-ray fluorescence) or electron (secondary or backscattered). A number of different detectors are used to produce various types of images. Images of the sample surface are obtained through use of the backscattered and secondary electron detectors. The backscattered electrons are generated from deeper within the sample and contain information that can provide chemical contrast. The secondary electrons, on the other hand, escape from the near surface regions and contain primarily topographical information. High resolution images of the capsule surfaces after deposition of each layer are shown in Figure 6. These are SEM images taken in secondary electron mode using a Hitachi S800 instrument. The number in the upper-right corner of each image indicates the number of layers that were deposited up to that point. These images were taken at a magnification of 1kX (scale bar = 50 μm). A clear progression in the surface roughness can be seen visually, and is particularly striking in the transition from the 4 layer to 5 layer sample. In the latter, the growth becomes extremely disordered and the resulting surface appears nodular rather than columnar. In fact, the beginnings of non-columnar growth are even seen in the 4 layer capsule. Further magnification to 5kX and 10 kX (Figures 7 and 8 respectively), shows this particular transition more noticeably. Interestingly, by comparing the images in Figure 8, it also appears that the grains on the surface become larger as the deposition process proceeds and further layers are added. To investigate this more fully, we plan to undertake a series of experiments in collaboration with LANL, where small sections (10x10μm) of several hundred nm thickness from each layer are made via FIB and subsequently studied with Transmission Electron Microscopy (TEM). This is the method of choice for determining grain structure and obtaining information on void size. It will be crucial to determine if these parameters can be correlated in any way with capsule strength.

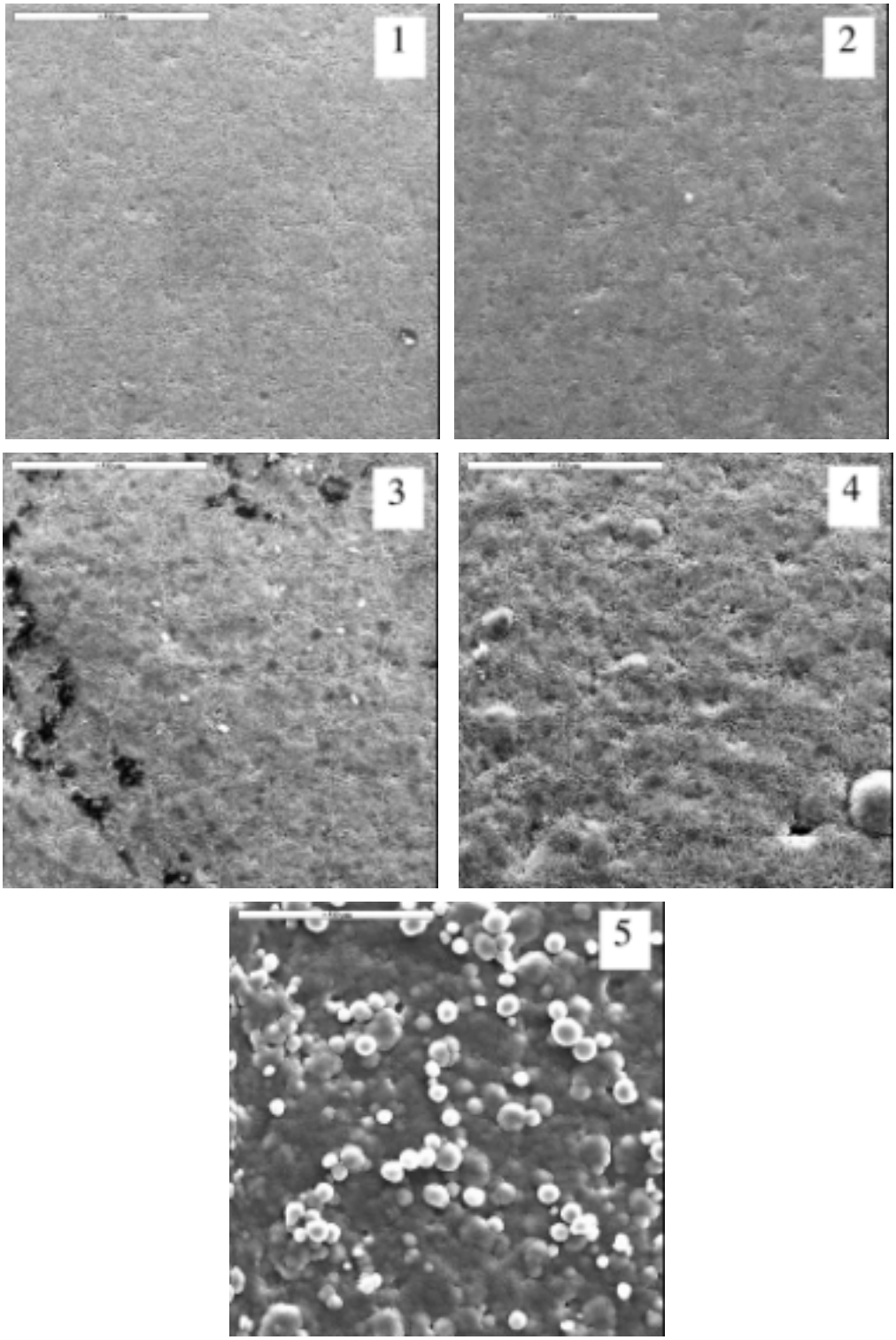


**Figure 6**. SEM images (secondary electron mode) showing the surfaces of a series of graded Cu-doped Be capsules. The number in the upper right corner indicates the number of layers that were deposited in each case. An increase in surface roughness as the deposition progresses is clearly shown in these images. The last image, a five-layer sample, shows nodular rather than columnar growth. (scalebar = 50 μm)

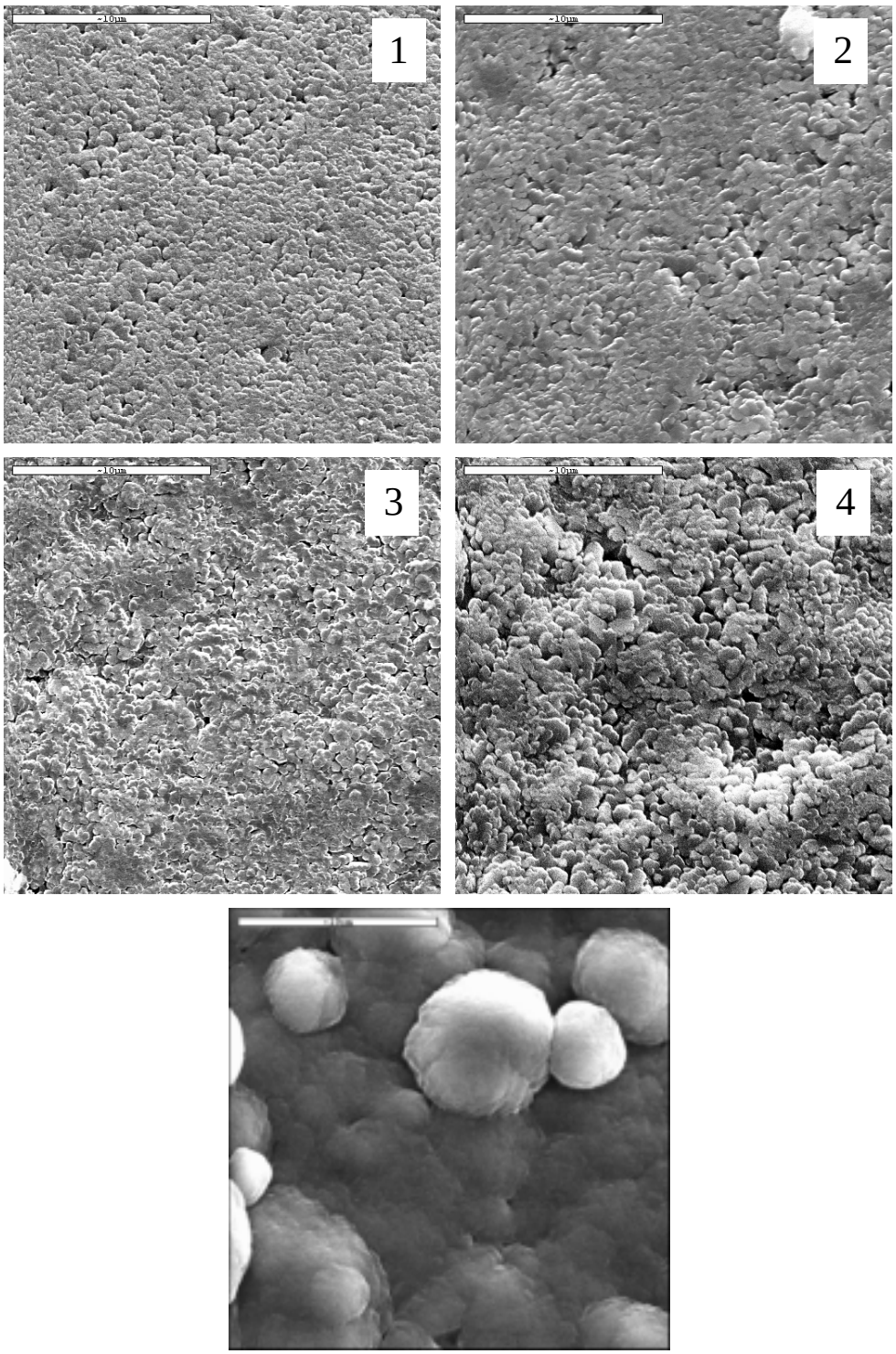


**Figure 7.** SEM images (secondary electron mode) showing further magnification of the graded capsule surfaces. (scalebar = 10 µm)

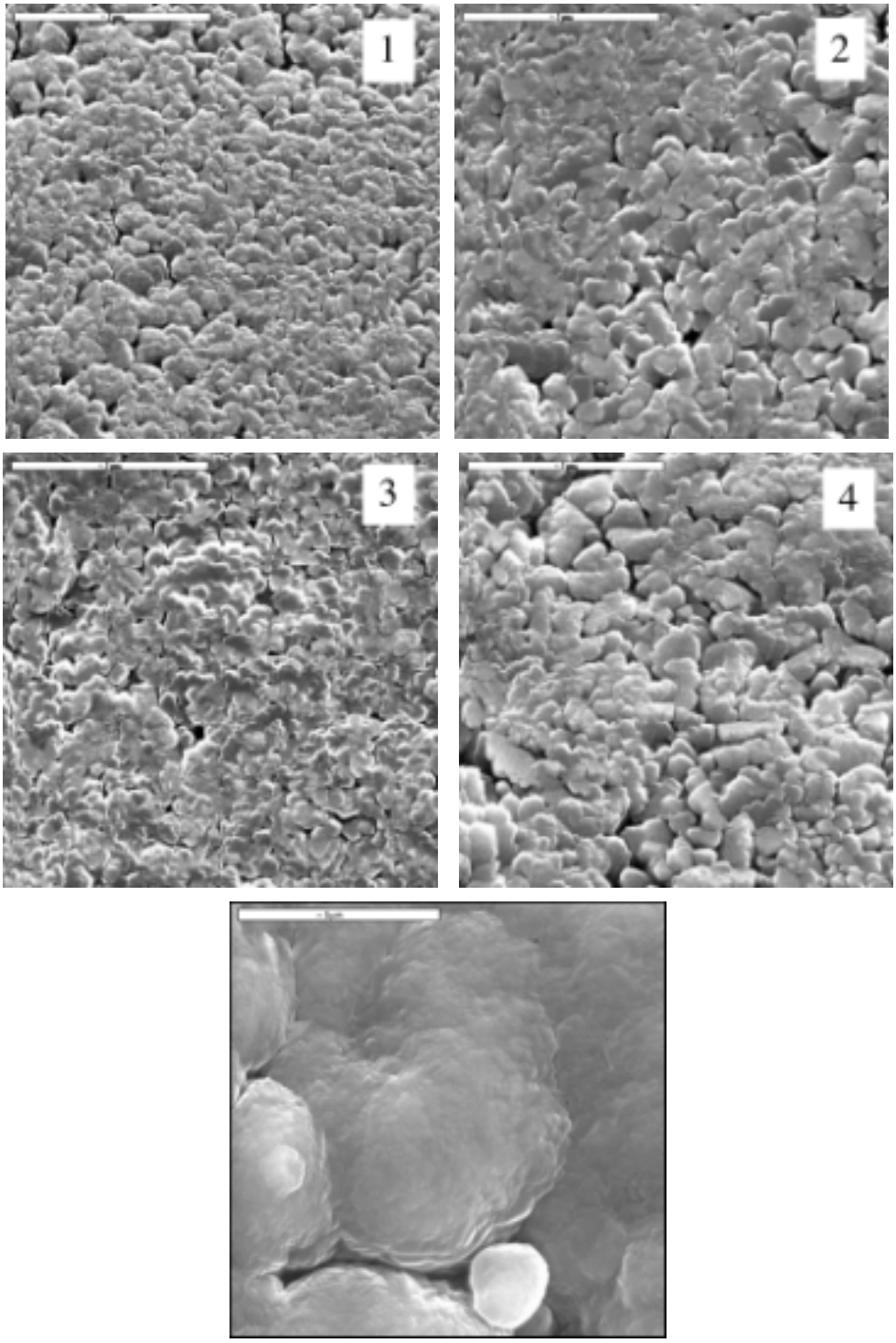


**Figure 8**. SEM images (secondary electron mode) showing further magnification of the graded capsule surfaces. The change in surface structure is very evident, particularly from layer 4 to layer 5 where the capsules began to stick to the bounce pan. (scalebar = 5 µm)

After the surface images of the capsule were obtained, the sample was fractured and re-examined in the SEM, so that information could be obtained on the internal structure, including both morphology, layer thickness, and chemical composition. Images of a fracture cross-section are shown in Figure 9. This was taken on a Hitachi S4500 SEM at an accelerating voltage of 4kV and 600x magnification in secondary electron mode. The first image shows the entire wall thickness along with a portion of the surface. Even without polishing, the 5 layers can be seen in the fracture cross-section. This is due in part to the fact that oxide is forming at the boundaries between the layers. This serves as a contrast mechanism in electron microscopy due to the higher atomic number of the oxides compared to pure Be. What is more interesting, however, is the fact that the growth seems to remain columnar until the last 5-10 μm. This is shown at a higher magnification in the second image of Figure 9. Some of the nodules are 10 microns or more in diameter and are poorly bonded to the surface as indicated by the arrows. The appearance of the nodules in the 5 layer capsules can be most easily explained by the fact that the capsules began to stick to the bounce pan at that point. The sticking phenomenon did not occur during deposition of earlier layers. Due to the fact that the 5 layer capsules are rough but not significantly out of round (i.e. a mode 2 problem), we know that the capsules are still turning periodically such that all parts of the surface receive additional sputtered material. However, the periodic sticking phenomenon appears to interfere with the growth process to the point where the resulting surface roughness exceeds even what can be measured via sphere-mapping (discussed later in this report).

Following fracture cross-sectioning, one half of the capsule was polished and embedded in epoxy for further SEM imaging to analyze the individual layers. An intact capsule is shown in Figure 10 along with an image of the capsule half prior to polishing and an image of the wall section after polishing. It is evident from the diffuse nature of the reflections in the first image that the extreme roughness can even be detected by eye. The second image shows the inner surface of the capsule that is pure Be and is shiny, indicative of a relatively smooth surface. The third image was obtained on a section of the wall using an optical microscope. The dark pits seen in the image are an artifact of the polishing process and not indicative of defects in the sputtered Be-Cu layers. Interestingly, all five layers can be seen in this image even though there is no mechanism in this particular experiment for detecting changes in chemical composition. The layers are detectable due to bands of oxide between them that most likely have a different response to mechanical polishing.

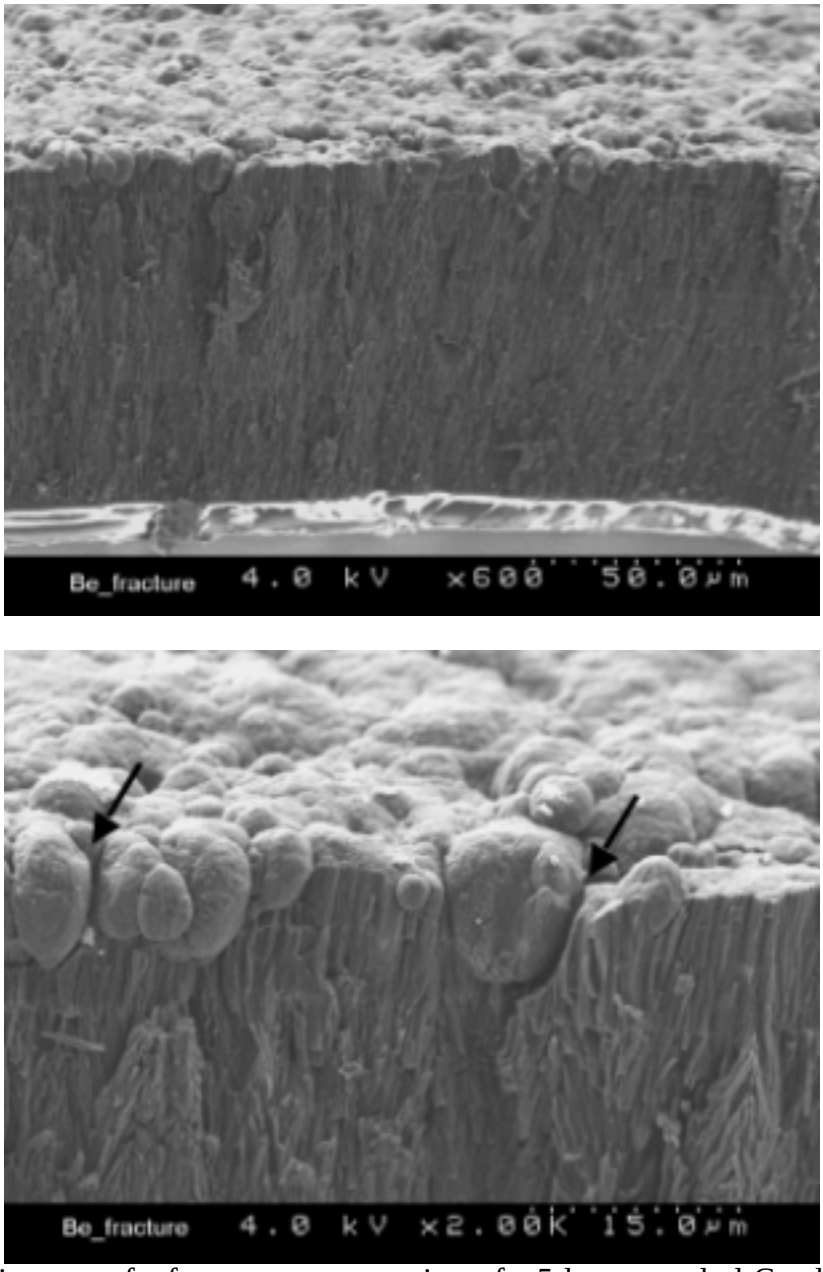


**Figure 9**. SEM images of a fracture cross-section of a 5-layer graded Cu-doped Be capsule. Evidence of columnar growth is seen through all but the last 5-10 microns on the outer surface. Some indication of intermediate layers is also seen. The magnified image also shows that the nodules formed in the outer layer are poorly bonded (see arrows).

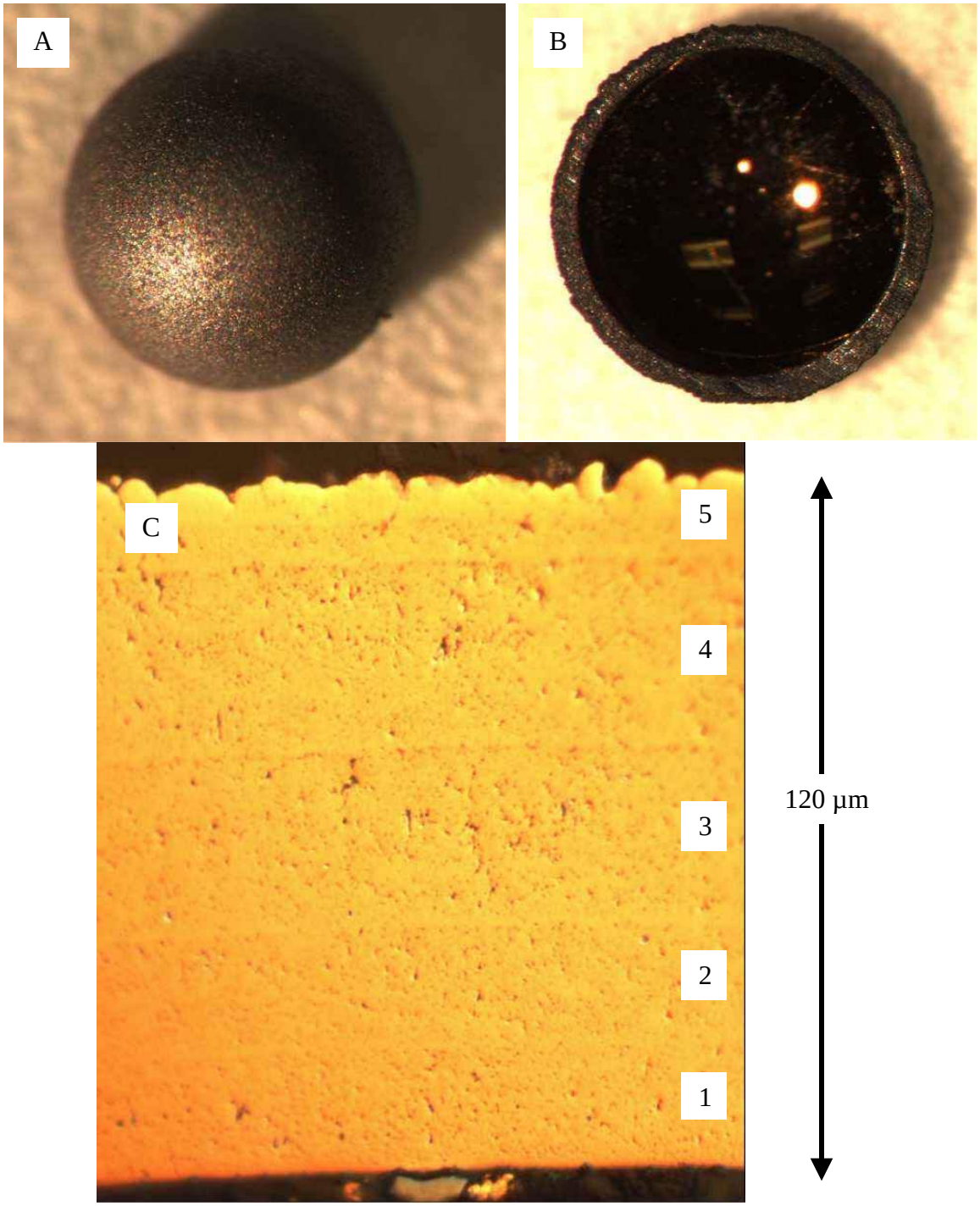


**Figure 10**. (A) An image taken by stereo microscope of a 5-layer graded capsule. The diffuse reflections show that the surface roughness can be easily detected even by eye. (B) The interior of a capsule that has been sectioned. The sharp reflections from the inner pure Be surface are suggestive of a much smoother surface. (C) Image of a capsule wall after cross-sectioning and polishing. Major layers can be seen by eye.

The corresponding SEM image of the polished cross-section is shown in Figure 11. This image was taken on a Hitachi S-4500 SEM at an accelerating voltage of 10kV at 1kX magnification in secondary electron mode. In general, secondary electron imaging contains both morphological and chemical information with an emphasis on the former. However, in this case since the image has been polished, the change in grayscale intensity across the wall is indicative of changes atomic number. The brighter regions correspond to higher concentrations of Cu, while the darkest areas correspond to pure Be layers. The thickness of each layer as measured is indicated on the figure and is in excellent agreement with the goals of the sputtering experiment. The bright lines that occur every 8-9 μm are also clearly seen in the SEM image. Analysis with EDS (energy dispersive spectroscopy) showed increased oxygen content in those regions. This suggests that there is enough background oxygen in the sputtering chamber, such that oxide builds up on the sputtering targets between deposition runs. This also implies that the initial material deposited is an oxide rather than either pure Be or Cu. Interestingly, for the first few days of deposition, the layers (as shown by the oxide interfaces) are relatively uniform. However they become significantly distorted after about 5 days of coating (see the 27 μm layer of nominal 0.70 at% Cu). Subsequent layers do not show the same pattern of distortions. Even more puzzling is the fact that these distortions seem to be self-healing, as indicated by the relatively undistorted boundaries between layer 3 and layer 4 (between day 7 and day 8 of deposition). It is not clear exactly why this occurs. However, it is suggestive perhaps of irregular grain growth or presence of voids (associated with the oxide) that disrupt the columnar structure. Further studies with TEM will investigate this in more detail. The oxide band effect may be reduced or eliminated with modifications that are currently being made to the sputtering system. By operating on a 24 hour schedule to minimize downtime and by using an ion-gun for cleaning, it may be possible to reduce the presence of oxide in the material deposited on the capsules. This in turn may also reduce some of the irregular intermediate surfaces seen in some of the initial layers.

To understand the changes in contrast seen in the SEM images, the same sample was analyzed with a JEOL Electron microprobe using a 15 keV, 20 nA beam focused into a 1-2 μm diameter spot. The sample was analyzed by wavelength dispersive x-ray spectrometry along a traverse from the outer circumference inward using a step size of 0.2 μm. Peak and background x-ray intensities were gathered at each point; x-ray intensities were converted to element atomic concentrations using a CITZAF algorithm. The size of the analysis area / excitation volume for most materials is on the order of 1 μm. Electron Probe Microanalysis (EPMA) is an analytical technique that combines high-resolution SEM imaging with quantitative and non-destructive elemental analysis of materials. This instrument can accommodate a wide variety of solid materials, including metals, ceramics, semiconductors, glasses and polymers. For the latter, which are generally non-conductive, a coating of Au or C is required. The detectable element range encompasses Be to U with detection limits of 10's to 100's of ppm.

The concentration profiles that were obtained for the 5 layer sample are shown in Figure 12. The first plot shows the concentration profiles for Be and Cu. The x-axis values range from slightly above zero at the outer wall to slightly over 80 μm at the inner wall. The total wall thickness analyzed in this experiment was approximately 80 μm. To minimize interference from the mandrel and from the roughness of the outer layer of pure Be, 5-10 μm on each side of the wall were not included in the analysis.

There are several notable features. First, the major steps in the Cu profile are evident, as are small peaks located at most of the sublayer positions (i.e. boundaries between daily deposition runs). With the current sputter system design, there are no shutters in front of the sputter targets. At the beginning of a run, the Cu target is at a higher power initially while that of the Be target is gradually ramped up. As a result, a small amount of Cu is actually deposited *before* the desired combination of Cu and Be is reached. This can be eliminated by adding shutters which will be done for the next version of the sputtering system. An additional feature in Figure 12A shows a noticeable decrease in Be content at the boundaries between layers 3 and 4 as well as 4 and 5. As can be seen in Figure 12B, these also correspond to regions where there is a significant increase in the oxygen content. These oxygen peaks correspond to points in the growth process where the chamber was opened to remove capsules.

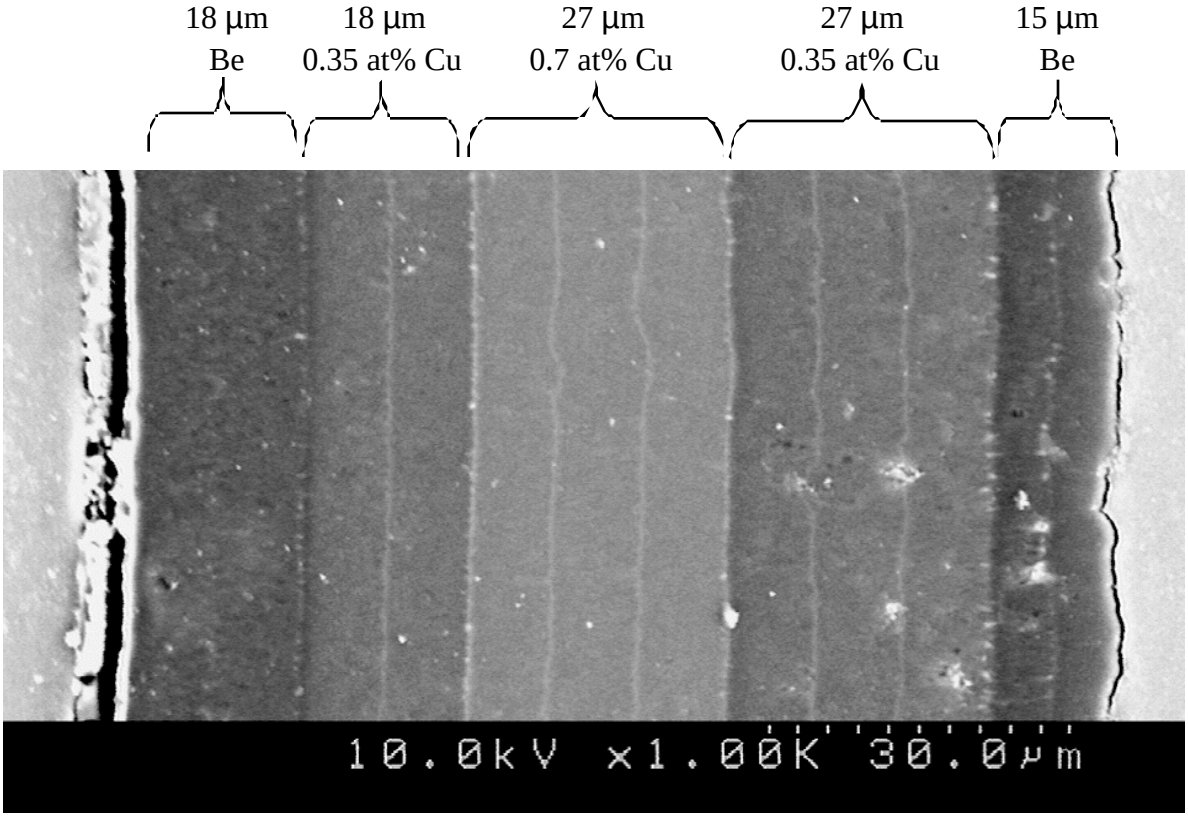


**Figure 11**. An SEM image of the polished cross-section shown in Figure 10c. The change in brightness across the wall is indicative of changes in atomic number. The brighter areas correspond to regions where higher atomic number species are present. The spacings are in good agreement with the goals of the sputtering experiment. The brightest lines (nearly white) occur approximately every 8-9 µm and represent the interface between daily runs. Analysis with EDS suggested increased oxygen content in these thin regions.

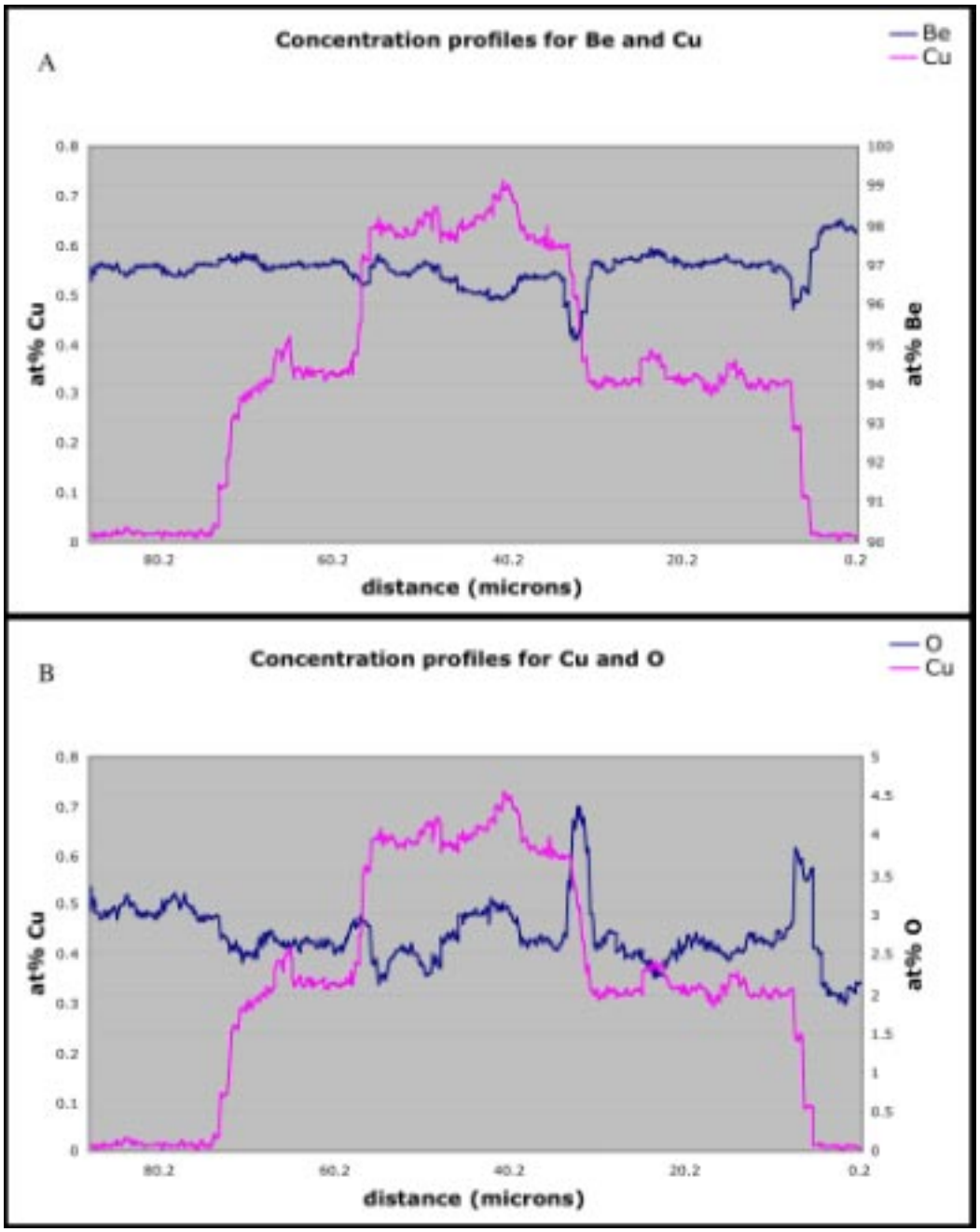


**Figure 12**. (A) Concentration profiles for Be and Cu. The steps between layers are shown clearly and occur at 0.33 and 0.65 at% Cu. Small peaks in the Cu content occur a significant percentage of the time in-between sputtering runs. (B) Concentration profiles for O, with Cu shown for comparison. Several large oxygen peaks are seen at the boundaries between layer 3 and 4 and layers 4 and 5 where the chamber was opened.

To best determine the concentrations of Cu within each layer, the histogram shown in Figure 13 was constructed using the data points analyzed in the line trace across the wall. The y-axis represents the number of points along the line scan while the x-axis represents the calculated Cu percentage for those points. Three peaks are seen in the histogram. The first occurs near zero which corresponds to the inner and outer

layers of pure Be (i.e. layers 1 and 5). Another peak occurs at a value of 0.35 at% Cu, while a third occurs at a value of 0.65 at% Cu. The second peak is higher than the third because there is a larger volume of Cu ( i.e. layers 2 and 4) compared with the third peak which represents only a single layer of Cu (i.e. layer 3). To verify these values, two shells were made, each with a single layer of Be-Cu at the two different doping levels used in the 5 layer capsule (i.e. nominally 0.35 and 0.70 at% Cu). These were analyzed via neutron activation. In this type of analysis, stable nuclides in the sample undergo neutron capture reactions when subjected to a flux of incident neutrons. The radioactive nuclides produced will generally decay by emitting a beta particle and gamma rays with a unique half-life. A high-resolution gamma ray detector is used for a quantitative analysis. The energies of the gamma-rays are used to determine what elements are present in the sample. The measured time dependent count rate of the gamma rays from the decay of a specific isotopes (in this case, Cu-64 with a half-life of 12.6 hours) in the irradiated sample can be related to the mass of the original isotope in the sample. Since we measured the mass of the shell before and after the deposition of the doped layer, we can determine the concentration of the dopant in the layer. We will express this as atom % Cu, determined as

$$\text{Atom \% Cu} = \frac{\mu\text{g Cu in sample} / 63.55}{\mu\text{g Be in sample} / 9.01 \; + \; \mu\text{g Cu in sample} / 63.55} \times 100 \qquad (1)$$

where the µg of Be is the mass of the layer minus the mass of the Cu in the layer. We have assumed no oxygen in the coating. The two lower Cu concentration samples were shown to contain 8.73 µg and 7.98 µg of Cu respectively, corresponding to 0.34 and 0.32 at% Cu. The two higher Cu concentration samples were shown to contain 15.9 and 17.3 µg of Cu, corresponding to 0.62 and 0.67 at% Cu. The average values are 0.33 and 0.65 at% Cu that is in excellent agreement with the results of 0.35 and 0.65 at% Cu obtained from the electron probe analysis.

Since surface roughness is a concern, sphere-mapping was performed on a representative shell after each layer was deposited. The results are shown in Figure 14. It is evident from the power spectrum that the shells become increasingly rough as additional layers are deposited. In fact, for layers 1 through 4, there is nearly an order of magnitude increase in power around mode 10 and nearly a two order change around mode 100. The 5 layer shell was too rough to be examined with the sphere-mapper. The peak to valley distance was out of the dynamic range of the instrument (approx 8 µm). Also on the graph is a curve corresponding to what is considered a “tolerable” surface, with no margins for other imperfections. It is clear from this comparison that the 4 layer shell is barely acceptable and that the 5 layer would most likely fail this particular specification. A curve that was obtained on polished Cu-doped Be flats shows that polishing may be a viable method for producing acceptable Cu-doped Be shells. This will be examined in FY05.

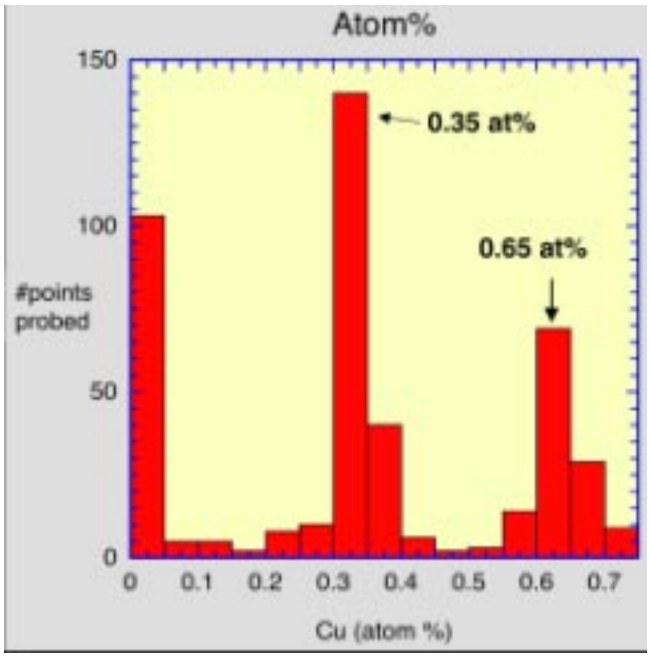


**Figure 13**. A histogram showing the dominant atomic concentration levels found in the sample. Over 400 points were sampled and the atomic percentage Cu determined at each point. The data points were then binned into 15 groups, each 0.05 at% wide and plotted in histogram form. Two peaks are seen, one at 0.35 at% Cu and another at 0.65 at% Cu. The peak corresponding to the lower concentration of Cu is substantially higher because the electron probe traverses more material at that concentration.

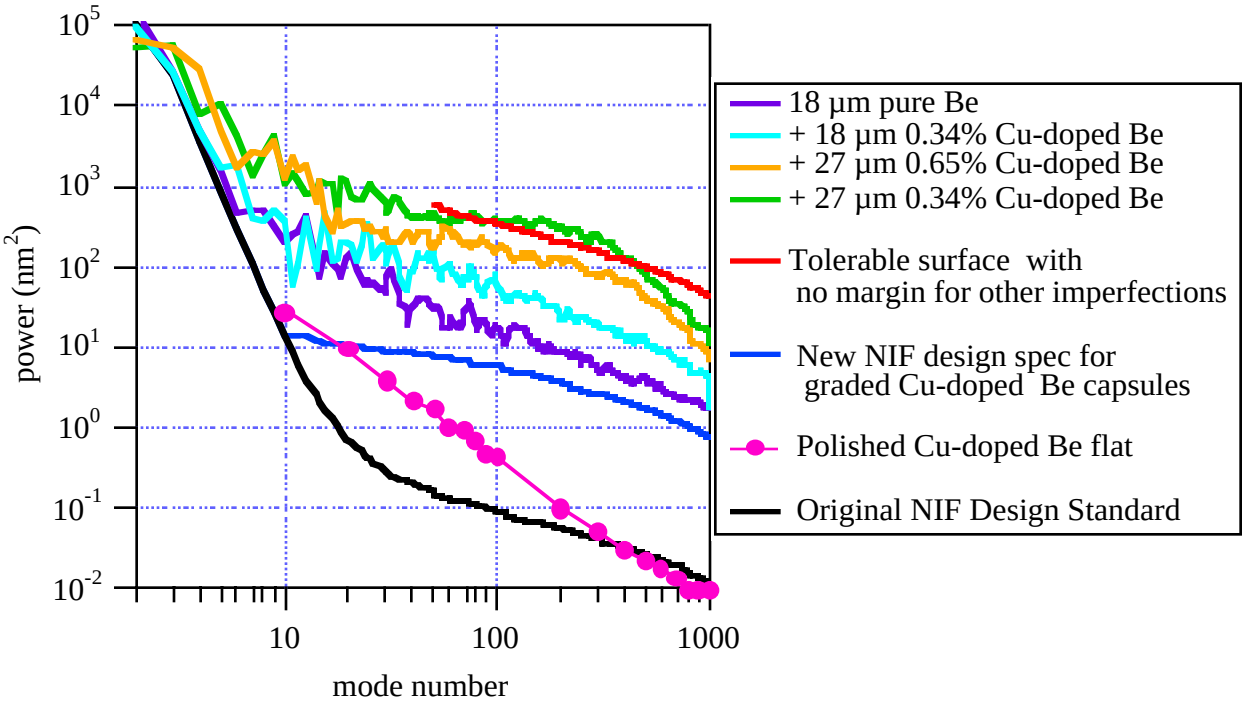


**Figure 14.** Shown are the successive sphere-mapping derived power spectra for the shells after each of the four layers was applied. Also shown is the new design (blue) as well as polishing results (pink).

All the techniques used thus far to analyze the graded shells were destructive. There is a strong impetus for developing a non-destructive technique for determining layer thickness and position. One possible solution is 2D radiography and Computed Tomography (CT). Traditional methods using film plates offer excellent resolution (i.e. submicron) but are time-consuming considering the procedures involved for preparing the sample chamber, pumpdown, and subsequent film development. In general, with the 2D radiography system at LLNL, 4-6 plates can be examined per day. There are commercial instruments that present the possibility of significant improvements in cost and flexibility while maintaining a resolution sufficient for analyzing graded shells. One such instrument is the Micro-tomography x-ray microscope, TXM-µXCT, manufactured by Xradia inc. This instrument operates in both low resolution and high-resolution mode which provides both 2.5 µm and 1.25 µm pixels respectively. A low-resolution image with a wide field of view is shown in Figure 15A. The capsule has been mounted on a thin glass pipette and attached by means of a small dab of glue, which can be seen towards the bottom of the image. Even in low resolution mode, it is possible to detect several of the layers visually (i.e. without the aid of computer analysis). A magnified portion of the wall in shown in Figure 15B. The mandrel is easily visualized, as are the first three layers. The third layer is the easiest to detect since it as the highest Cu content and therefore the highest opacity (darker gray value in this case). It is difficult to distinguish between the last two layers, partly because these interfaces are more rough. However, upon careful examination, it is possible to find the boundary by visual inspection of the radiograph.

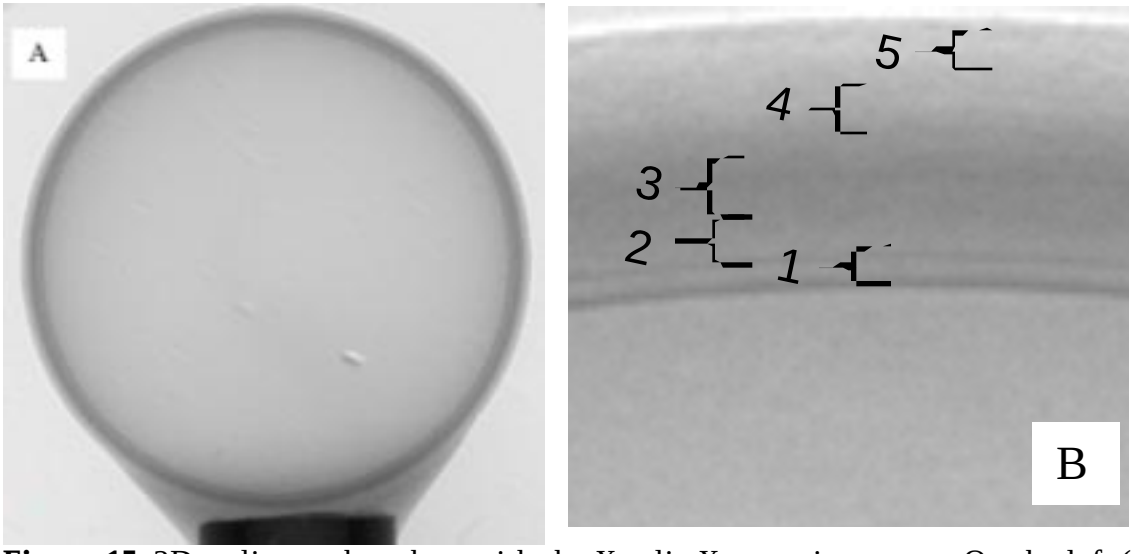


**Figure 15.** 2D radiographs taken with the Xradia X-ray microscope. On the left (A) is a low-resolution image of a 5 layer capsule mounted on a thin glass rod. Pixel size is approximately 2.5 µm. On the right (B) is a portion of the capsule wall taken from the image in (A) above. The mandrel is easily visualized along with several of the subsequent layers.

A high resolution radiograph of the same capsule is shown in Figure 16. The smaller pixel size (~1.25 µm) makes it slightly easier to detect the layers. With this instrument, since the sample is not in direct contact with the detector (as it is in film radiography), the resulting image is a combination of absorption and phase contrast.

With the Xradia instrument, one can change the sample to detector distance and thus the amount of phase contrast in the image. Figure 16 represents an attempt to maximize the amount of phase contrast in order to highlight the layer boundaries as much as possible. The first three layers remain easy to detect, while there is also a slight improvement in the ability to detect the boundary between the last two layers. One of the most notable features of the image however, is the fact that even the sublayers can be seen quite easily. The thin bands within a given layer are spaced at approximately 9 μm which is in good agreement with the sublayer spacing determined via SEM analysis of the cross-section.

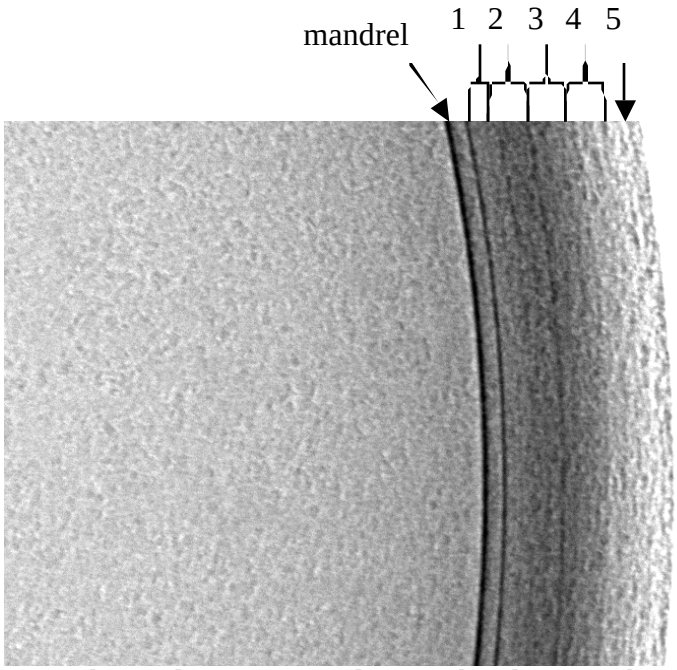


**Figure 16**. High resolution 2D radiograph taken on the same 5 layer capsule with the Xradia X-ray microscope. The 5 layers are indicated in the figure. Finer spacings can be seen in the image as a result of phase contrast. These represent the amount of material deposited in a single session (i.e. 8-9 μm).

To fully evaluate the ability of radiography to determine layer spacings, it is critical to perform a computer analysis to look at both the transmission and its second derivative as a function of radial position. The second derivative of the transmission should, in an ideal situation with perfectly sharp boundaries, exhibit sharp peaks at each layer boundary. As the boundaries become less distinct due to various factors including roughness, the peaks in the second derivative become broader. Figure 17 shows a radially averaged lineout for a 5 layer graded Cu-Be capsule that was produced via software developed at General Atomics. The line at the top represents the transmission across the wall, averaged radially, where the y-axis represents a grayscale value and the x-axis represents the pixel position. The large peaks on either end of the curve represent the inner and outer boundaries (i.e. the outside layer and the mandrel). The subtle slope changes in the transmission curve (selected ones are marked with arrows) are locations of the individual layers. The line at the bottom of the figure shows the second derivative of the intensity. The inner and outer boundaries are seen also as peaks, but have been broadened as a result of phase contrast issues as well as surface roughness. The small peaks in the middle portion of the curve represent the sublayers deposited in

a single day. These are well above the noise level and are real features. Computer analysis of these images suggests that the layer spacing can only be determined to within 2-3 μm, at least for these particular experimental conditions and resulting images. These results indicate that radiography is a promising technique for non-destructive analysis of graded shells. However, further improvement is critical, since there is a need to determine the layer thicknesses and positions to less than a micron.

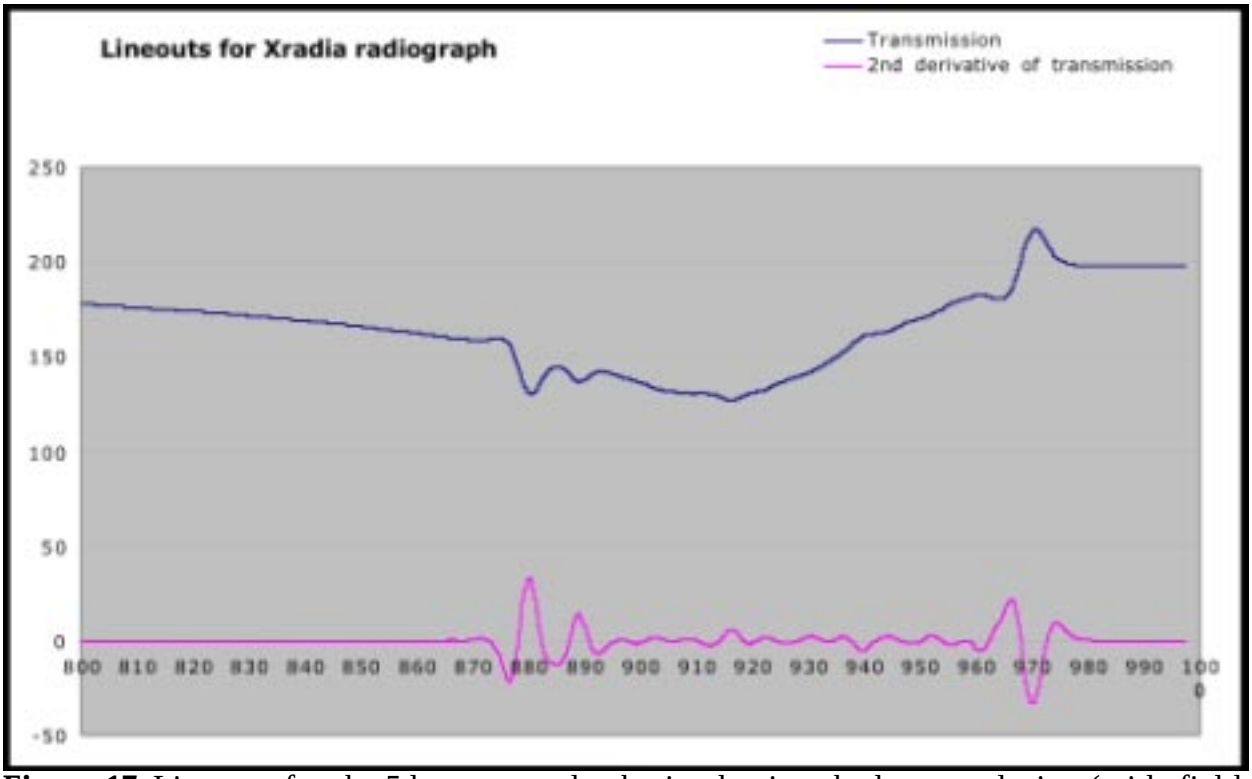


**Figure 17**. Lineouts for the 5 layer capsule obtained using the low-resolution (wide field of view) radiograph taken with the Xradia X-ray microscope. The Blue line (top) represents the transmission across the wall. Subtle changes in slope help indicate the layer position. The pink line (bottom) represents the second derivative of the intensity. The peak positions are generally more practical to use for identifying layer positions compared with the slope changes in the transmission curve. The inner and outer surfaces are easily identified. The inner layers, and also the sublayers (representing a single day's deposition), are seen as smaller peaks.

**Summary**

On balance our first attempt was very successful. Not only did we succeed in laying down 5 successive layers of approximately the right concentration of dopant to make a shell with about a 100-μm wall, but equally important we highlighted numerous problems with the fabrication and characterization techniques that we can address with potential solutions in our next multi-layer thick gradient Cu-doped Be shell coating. Attempting (unfortunately unsuccessfully!) to preparing 0.5 mm gas filled capsules for Omega shots in mid October has occupied us until late September, but we expect to get back to Be coatings in early October, with the first efforts to install and test out the

effects of an ion gun on the coating morphology. Another thick, multi-layer capsule run should commence in late October.

**Acknowledgements**

The authors would like to thank the following individuals for their contributions to this work: Evelyn Fearon for Sphere-mapping, James Hughes for XRF measurements, Edward Lindsey for SEM and EDS, and Charlotte King for assistance with contact radiography. Other individuals who contributed were Mark Wall and Richard Gross for SEM sample preparation, Jim Ferreira for additional SEM imaging and Frederick Ryerson for EPMA work. David Scott of Xradia Inc. provided contact radiography and CT instrumentation used to produce images of the graded Cu doped Be capsules. Larry Kovar of General Activation Analysis, Inc. for providing Neutron Activation analysis.